

# Background Studies of a Position Sensitive CdZnTe X-ray Detector at Balloon Altitudes

K. Slavis<sup>1</sup>, P. Dowkontt<sup>1</sup>, F. Duttweiler<sup>2</sup>, J. Epstein<sup>1</sup>, P. Hink<sup>1</sup>, G. Huszar<sup>2</sup>, P. Leblanc<sup>2</sup>, J. Matteson<sup>2</sup>, R. Skelton<sup>2</sup> and E. Stephan<sup>2</sup>

<sup>1</sup>*Dept. of Physics, McDonnell Center for the Space Sciences, Washington Univ., St. Louis, MO 63130*

<sup>2</sup>*Center for Astrophysics and Space Sciences, University of California - San Diego, La Jolla, CA 92093*

## Abstract

Cadmium Zinc Telluride (CZT) is a room temperature semiconductor detector well suited for high energy X-ray astronomy. We flew a position sensitive CZT detector on two balloon flights as part of the High Energy X-ray Imaging Spectrometer (HEXIS) development program to demonstrate CZT's good energy resolution, spatial resolution and low background in a realistic cosmic ray environment. Passive, active and hybrid passive-active shields were used both with a cross-strip detector and a standard planar detector. The cross-strip detector utilized our recently developed, novel electrode configuration that improves interaction localization and depth of interaction (DOI) determination. Results of background levels, shield rejection effects and upper limits on CZT activation are presented. Based on our preliminary analysis, we are confident that CZT detectors will be desirable for future low background, hard X-ray astronomy missions.

## 1 Introduction:

The most recent hard X-ray all-sky survey was in 1978 with HEAO-1/A4. This survey was conducted for 13-80 keV at a sensitivity of 13 mCrab (Levine, et. al., 1984). Subsequent hard X-ray missions have conducted pointed observations of known sources or lower sensitivity all-sky monitoring. The High Energy X-ray Imaging Spectrometer (HEXIS) all-sky survey mission concept (Matteson, et. al., 1998) is based on the detectors described in this paper. HEXIS will have 25 times higher sensitivity than HEAO-1/A-4 with sub-degree angular resolution, few keV energy resolution and sub-millisecond time resolution. Astrophysical topics of interest include gamma-ray bursts, black holes, pulsars, and active galactic nuclei. Overall, HEXIS's objectives are to improve our knowledge of the high energy X-ray sky by increasing the number of known sources above 20 keV, discovering transient sources and conducting spectral and temporal studies of these sources. In addition CZT will be valuable as a focal plane imager on hard X-ray focusing optic missions, such as Constellation X and Far-XITE (Rothschild, et. al., 1998).

CZT is a room temperature semiconductor detector having very good energy resolution, 5 keV @ 60 keV, and very fine spatial resolution, 50  $\mu\text{m}$  at 22 keV and 100  $\mu\text{m}$  at 88 keV (Matteson, et. al., 1997) while maintaining good detection efficiency from 5-200 keV. The combination of these properties, ease of packaging, the modest number of channels required with strip detectors, and no gas or cryogenics requirements, yields advantages over scintillators, high pressure gas, Si and Ge detectors. CZT is suitable for both large area survey missions (HEXIS) and for use as focal plane detectors for hard X-ray focusing optics (Far-XITE). In this work we are investigating CZT's background characteristics and the feasibility of using it successfully to conduct these various missions. Our results indicate that CZT's background level is suitable for these missions.

## 2 Instrument Description:

We flew two detectors on two balloon flights from Ft. Sumner, NM in October 1997 and May 1998. The first detector is a position sensitive orthogonal strip detector with 500  $\mu\text{m}$  pitched anodes and cathodes. The anode electrodes are 100  $\mu\text{m}$  wide with 150  $\mu\text{m}$  gap and a 100  $\mu\text{m}$  wide interleaved steering electrode.

The cathode electrodes are 450  $\mu\text{m}$  wide with 50  $\mu\text{m}$  gap. This detector has 22 anodes, 22 cathodes and one multi-strip steering electrode. Due to a limitation in the number of readout channels available, 8 individual anode strips and 7 individual cathode strips were readout. The remainder of the anodes and cathodes were coupled to 4 readout channels. The second detector is a planar detector with the same active area as the cross-strip detector and was flown for comparison with results in the literature. Both detectors are discriminator grade, 1.1 cm x 1.1 cm x 2 mm, manufactured by eV products with a 200 V bias applied.

The cross-strip CZT electrode geometry, as described above, has been optimized for energy resolution and 3-D position resolution. The wide cathodes are sensitive to charge induction deep into the detector, resulting in better charge collection and depth of interaction sensitivity. The narrow anodes concentrate most of the charge development near the anode, reducing sharing between anodes and improving photopeak efficiency. Charge sharing is also reduced on the anodes by the steering electrode, which is held at 10% lower bias with respect to the anodes. The steering electrode directs charge onto an anode and recovers energy deposition information normally lost with deeply interacting events (Matteson, et al., 1998, Slavis, et al, 1998). This novel design allows us to use discriminator grade material with spectroscopic grade performance. We use hole trapping to our advantage by inferring the depth of interaction of X-rays allowing rejection of rear and side entrant events at lower energies. As we reduce the noise in the system with application specific integrated circuits (ASICs), we will be able to more accurately determine the depth of interaction.

The first flight (1997) utilized  $4\pi$  sr passive PbSnCu shielding in two thicknesses – 7mm, 2mm, and no shielding; data from that flight have been presented by Slavis, et al., 1998. The second flight had four active and hybrid passive-active shielding configurations. The first shield configuration for the 1998 flight is 5.5 cm thick CsI side and rear shielding with an 8 cm thick 20° FOV NaI collimator, covered by a 2 mm graded PbSnCu shutter. The second configuration has the shutter removed. In the third configuration the NaI collimator is replaced with a passive 2 mm thick PbSnCu collimator with the same FOV. In the fourth configuration only the side and rear CsI shields were used, resulting in a 140° FOV. The changes in the shield configuration were performed by radioed commands to the package. The 1998 flight has 22 hours of data at float altitude.

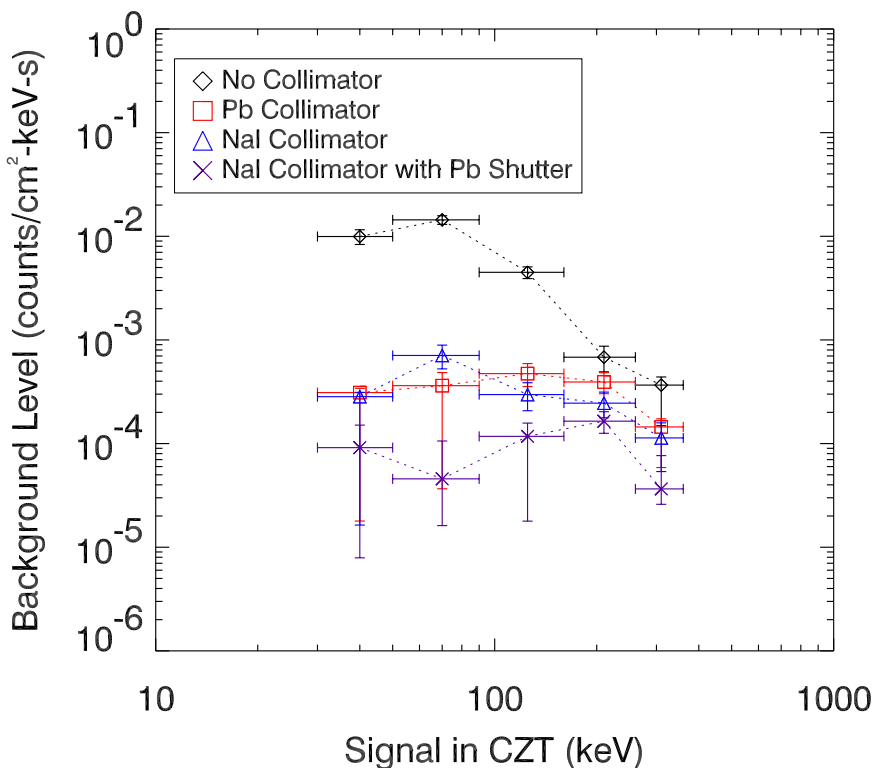


**Figure 1:** Background levels in CZT cross-strip with CsI side and rear shielding and various collimators. Shield anticoincidence and other rejection techniques have been applied.

### 3 Background Levels at Float:

We have examined the central 30-pixel region for the four shielding configurations from the May 1998 flight and show the corresponding background levels in figure 1. Events with greater than 50 keV of energy deposition in the shield have been rejected. It is interesting to note that the NaI and PbSnCu collimators give equivalent results, indicating that most of the background reduction is achieved by the rear and side active shields. The difference between data with the PbSnCu shutter on and off give the atmospheric flux, and are consistent with expected levels. We find the background to be  $9^{+6}_{-8} \times 10^{-5}$  cts/cm<sup>2</sup>-s-keV in the 30-50 keV energy range and  $5^{+6}_{-3} \times 10^{-5}$  cts/cm<sup>2</sup>-s-keV in the 50-90 keV energy range using the full active shield with a PbSnCu shutter over the aperture. These background levels are suitable for sensitive hard X-ray surveys or for the focal plane of X-ray focusing instruments.

### 4 Shield Effects:

We telemetered the pulse heights of the active shields' photomultiplier tubes (PMTs) for each CZT triggered event. From these data we are able to study the effect of the shield energy threshold on the background seen by the CZT. The plot in figure 2 is the background level in the central 30 pixels of the cross-strip detector after rejecting events where any one of the three shields had an energy deposition of the

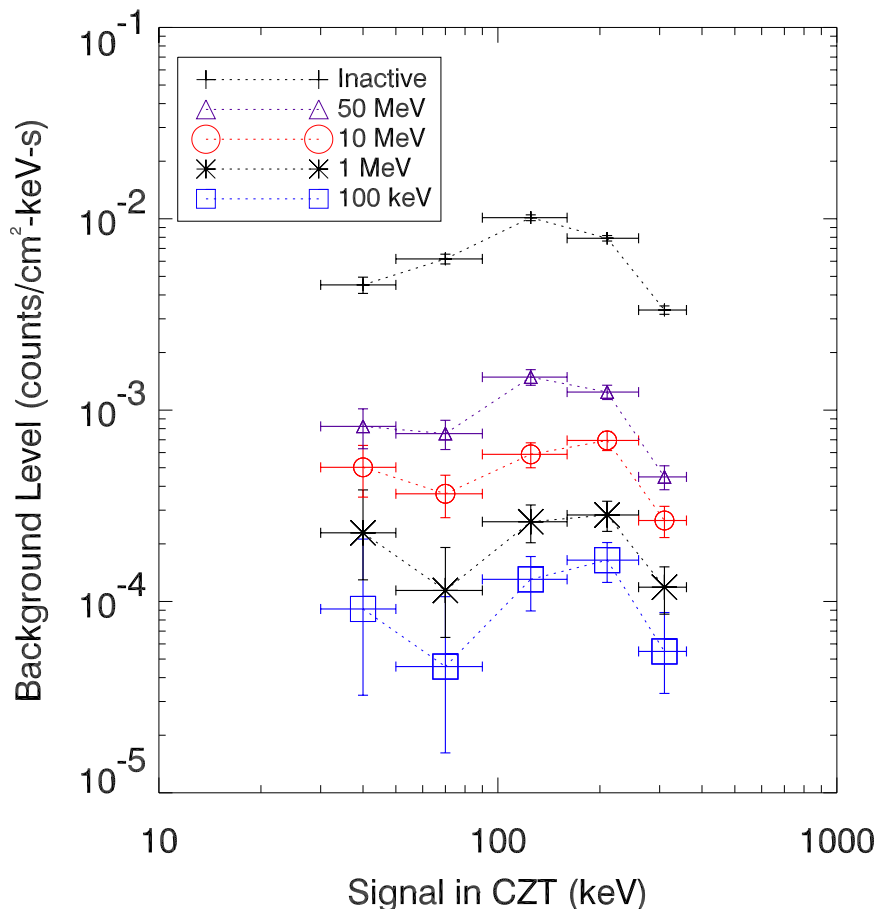
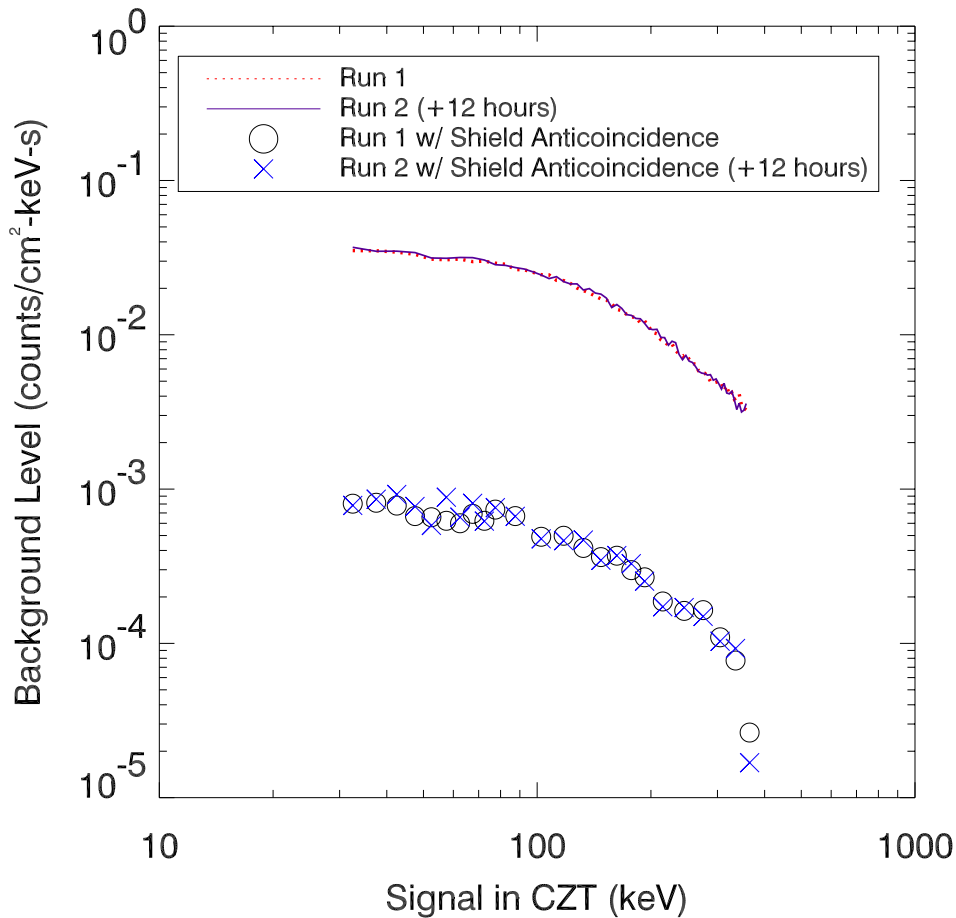


**Figure 2:** Effect of the active shield threshold level on cross-strip CZT background for the NaI collimator with a PbSnCu shutter shield configuration.

selected threshold or higher. Using a threshold of 50 MeV rejects some of the coincident cosmic rays, whereas a threshold of 10 MeV rejects most of the cosmic rays given the path length distribution and gradients in the shield. A threshold of 100 keV is approximately our shield sensitivity limit. The background generated by the cosmic rays is the predominant component in the data. We will use plastic scintillators to reject this component in the HEXIS design and expect background levels in HEXIS to be comparable to the 10 MeV threshold data in figure 2,  $\sim 5 \times 10^{-4}$  cts/cm<sup>2</sup>-s-keV at 30-100 keV. The next HEXIS test flight will be configured with a plastic scintillator and a PbSnCu shield to verify this.

## 5 Activation:

We have investigated activation of CZT by comparing two data sets taken twelve hours apart. In figure 3, we plot the data for the NaI collimator with the PbSnCu shutter closed. Due to the higher statistics available with the planar CZT detector, we use it rather than the cross-strip detector for investigation of any signs of activation. We hope to obtain comparable or better statistics for the cross-strip detector on a



subsequent balloon flight. Since activation resulting in high energy gamma rays would be rejected by the anticoincidence shield, it is instructive to analyze the data by treating the shields as passive materials (solid and dotted lines in figure 3). Using the shield to actively reject background, we are more sensitive to low energy activation (O and X data in figure 3). In neither case do we see any evidence of activation within the planar detector over a course of twelve hours to a level of  $< 3 \times 10^{-4} \text{ (cm}^2\text{-s-keV)}^{-1}$  with an active shield and  $< 10^{-3} \text{ (cm}^2\text{-s-keV)}^{-1}$  with a passive shield.

**Figure 3:** Activation study for shield configuration NaI collimator, PbSnCu shutter closed. Typical error bars are comparable to the size of the symbols and lines, correspondingly.

## References

- Levine, et al., 1984, ApJS, 54, 581.
- Matteson, J., et al., 1997, SPIE Proc., 3115, 160.
- Matteson, J., et al., 1998, SPIE Proc., 3446, 192.
- Matteson, J., et al., 1998, SPIE Proc., 3445, 445.
- Rothschild, et al., 1998, AAS, 192.3505.
- Slavis, K., et al., 1998, SPIE Proc., 3445, 169.
- Slavis, K., et al., 1999, SPIE Proc., submitted.